

# A novel scheme for synchronous optical sampling based on multicast parametric process\*

WANG Tao (王涛)<sup>1\*\*</sup>, ZOU Jia-xiu (邹佳琇)<sup>2</sup>, MEI Chao (梅超)<sup>1</sup>, ZHANG Xian-ting (张显廷)<sup>1</sup>, YUAN Jin-hui (苑金辉)<sup>1</sup>, and YU Chong-xiu (余重秀)<sup>1</sup>

1. State Key Laboratory of Information Photonics and Optical Communications, Beijing University of Posts and Telecommunications, Beijing 100876, China

2. School of Electronic Engineering, Beijing University of Posts and Telecommunications, Beijing 100876, China

(Received 18 October 2014)

©Tianjin University of Technology and Springer-Verlag Berlin Heidelberg 2015

We propose a novel scheme for synchronous optical sampling based on multicast parametric process. The linearly chirped and time-broadened pulses are utilized to replace the traditional mode-locked sampling pulses. An optical sampling rate of 80 Gbit/s is realized by using only one sampling source with repetition rate of 10 GHz.

**Document code:** A **Article ID:** 1673-1905(2015)01-0053-4

**DOI** 10.1007/s11801-015-4192-1

With the rapid development of optical communications, various professional applications based on high-speed data service can meet more and more demands of people, such as three-dimensional movies, advanced radar systems and real-time signal monitor. Researchers have paid much attention on high-speed signal processing, and many smart schemes have been proposed<sup>[1-6]</sup>. In the previous schemes, the preprocessing was added in both electronic and optical domains. Because of the inherent electronic bottleneck of electrical devices, the speed of signal processing is limited. All-optical signal processing can successfully overcome the electronic limitation, and has been extensively studied in high-speed signal processing applications<sup>[7-10]</sup>. All-optical sampling is one of the most important parts of all-optical signal processing. Brès et al<sup>[11]</sup> have demonstrated the synchronous sampling scheme with optical multicast, which is achieved in optical domain. However, there is a shortage that the high-speed input signals need high repetition rate for the mode-locked laser, which is very difficult and expensive. It can be solved by generating lots of copies previously<sup>[12,13]</sup>, but it will lead to more complex structure and larger parametric gain bandwidth.

In this paper, we propose a novel scheme of synchronous optical sampling based on multicast parametric process. The original sampling pulses are replaced by the broadened and linearly chirped pulses, which can solve the problem mentioned above successfully. The corresponding numerical analyses and simulations are dis-

cussed to prove the feasibility of our scheme.

Fig.1 shows the signal parametric multicast and time delay blocks. 4 multicast parametric channels are utilized as example, which are generated in the highly nonlinear fiber (HNLF1) based on parametric process. The idler gain is given as

$$G \propto \exp[2\gamma L_1 E_p(t)], \quad (1)$$

where  $G$  is the idler gain,  $\gamma$  is the nonlinear coefficient,  $L_1$  is the length of HNLF1, and  $E_p(t)$  is the power of pump signal. Here, the envelopes of 4 idler signals change with the envelope of pump signal, and the 4 copies are time delayed in a single mode fiber (SMF). Compared with the pulse center of pump in the process of parametric sampling, the temporal delays between pump and Copy 1, Copy 2 are set to be  $-T_{NRZ}/2$ ,  $-T_{NRZ}/4$ ,  $T_{NRZ}/4$  and  $T_{NRZ}/2$ , where  $T_{NRZ}$  is the period of the non-return-to-zero (NRZ) signal. Thus, the center of the pump can temporally overlap with the whole temporal range of one NRZ code.

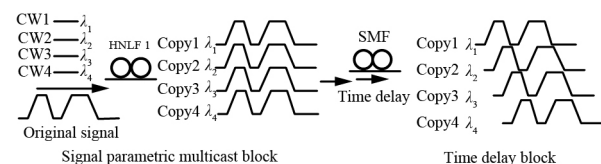


**Fig.1 Schematic diagram of signal multicast and time delay blocks**

\* This work has been supported by the National Natural Science Foundation of China (Nos.61475023, 61307109 and 61475131), the National High Technology Research and Development Program of China (No.2013AA031501), the Specialized Research Fund for the Doctoral Program of Higher Education (No.20120005120021), the Fundamental Research Funds for the Central Universities (No.2013RC1202), the Program for New Century Excellent Talents in University (No.NECT-11-0596), the Beijing Nova Program (No.2011066), and the Fund of State Key Laboratory of Information Photonics and Optical Communications.

\*\* E-mail: wangtaoseasky@163.com

The time-broadened and linearly chirped pulses are obtained via a dispersive fiber, as shown in Fig.2(a).The time-dependent phase variation of the chirped pulse is expressed as

$$\phi_p(z,T) = -\frac{\text{sgn}(\beta_2)(z/L_D)}{1+(z/L_D)^2} \frac{T^2}{2T_0^2} + \frac{1}{2} \arctan(z/L_D), \quad (2)$$

where  $T_0$  is the initial full width at half maximum (FWHM) of the sampling pulse,  $L_D$  is the dispersion length, and  $\beta_2$  is the second-order dispersion coefficient of the fiber. The chirped pulses are utilized as pump and delivered into another HNLF together with 2 signal copies ( $n=1, 2, 3, 4$ ) to realize the parametric sampling process. Because of the phase combination of the pump pulses  $A_p(t)$  and the signal copies  $A_{s,n}(t)$  during the parametric process, the phase of the idler signal  $A_i(t)$  is modulated by the chirped pulses<sup>[14,15]</sup> as

$$\phi_i(z,T) = 2\phi_p(z,T) - \phi_{s,n}(z,T). \quad (3)$$

Compared with the chirp of pump, the chirp of signal copies can be neglected. Thus, the frequency variation of the idler signal is

$$\delta\omega_i(T) = -2 \frac{\partial\phi_p}{\partial T} = \frac{2 \text{sgn}(\beta_2)(z/L_D)}{1+(z/L_D)^2} \frac{T}{T_0^2}. \quad (4)$$

It can be seen that the chirp of idler signals is not only linear, but also twice as many as that of the pump signal, which is also shown in Fig.2(b).

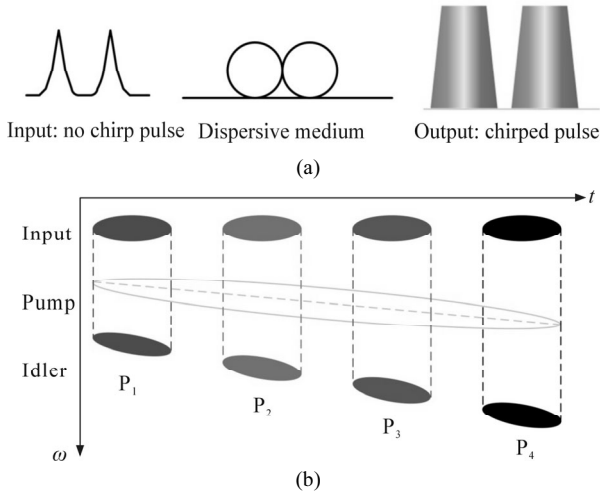


**Fig.2 (a) Time-broadened and linearly chirped pulses and (b) the chirp of idlers ( $P_1$ - $P_4$  correspond to four sampling points.)**

The parametric sampling based on four-wave mixing (FWM) in HNLF2 is shown in Fig.3. The sampling points in time domain can be extracted by filtering out different frequency components of the generated idlers, which is implemented by the arrayed waveguide grating (AWG) in our scheme. Further, the extracted sampling points are delivered into the signal processing block for equalization and coding.

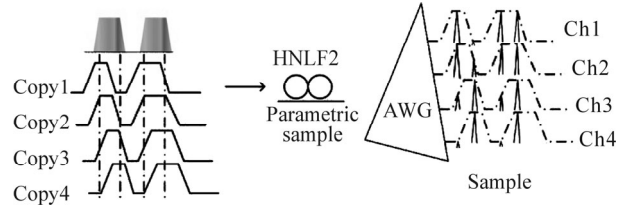


**Fig.3 Schematic diagram of the parametric sampling block based on FWM**

The equivalent sampling rate can be calculated by

$$R = \frac{|\delta\omega_i(T)|_{\max} nR_p}{\Delta H}, \quad (5)$$

where  $\Delta H$  is the bandwidth of the fiber,  $n$  is the number of copies, and  $R_p$  is the repetition rate of the pump pulse train. Since  $nR_p$  is the sampling rate in previous schemes, it is evident that the sampling rate  $R$  can be improved if the ratio satisfies  $|\delta\omega_i(T)|_{\max} / \Delta H > 1$ . Hence, the proposed scheme has great advantages in enhancing the sampling rate over the previous schemes.

Based on the theoretical analysis above, the schematic diagram of our proposed scheme is shown in Fig.4. In block A, the original pump source is centered at 1 550.4 nm and intensity modulated by a 10 Gbit/s NRZ bit sequence. Before being multiplexed with continuous waves of CW1–CW4 with the same power of 1 dBm and wavelengths of 1 536.3 nm, 1 538.1 nm, 1 540.0 nm and 1 542.0 nm in a wavelength division multiplex (WDM), the pump signals are amplified by an erbium-doped fiber amplifier (EDFA1) and filtered by a 0.6 nm optical band pass filter (BPF1) to eliminate the amplified spontaneous emission noise. The HNLF1 is followed as the nonlinear medium to generate the 4 copies, which is known as the parametric multicast. The length, attenuation coefficient, zero dispersion wavelength (ZDW) and dispersion slope at ZDW of the HNLF1 are 100 m, 0.9 dB/km, 12  $W^{-1}\cdot km^{-1}$ , 1 549.5 nm and 0.022 ps/( $nm^2\cdot km$ ), respectively. An 8 nm BPF2 is placed after HNLF1, which can remove the original pump signals and CW1–CW4. Copy1–Copy4 are further delivered into a 1 200 m standard single-mode fiber (SSMF) to get the temporal time delay. In block C, a 10 GHz Gaussian pulse train at 1 555 nm with the pulse width of 10 ps is used as the sampling source. The sampling pulse train is linearly chirped in a 5 km SSMF and amplified by the EDFA2. The parameters of EDFA2 are the same as those of EDFA1, which has the maximum output power and the noise figure of 30 dBm and 4 dB, respectively. The BPF3 is used to filter out the linearly chirped pump. The HNLF2 is used for the parametric sampling process. The attenuation coefficient, nonlinear coefficient, ZDW and dispersion slope at ZDW of HNLF2 are 0.9 dB/km, 12  $W^{-1}\cdot km^{-1}$ , 1 553 nm and 0.02 ps/( $nm^2\cdot km$ ), respectively. By the proper design of AWG placed after HNLF2, the desired sampling points can be extracted accurately.

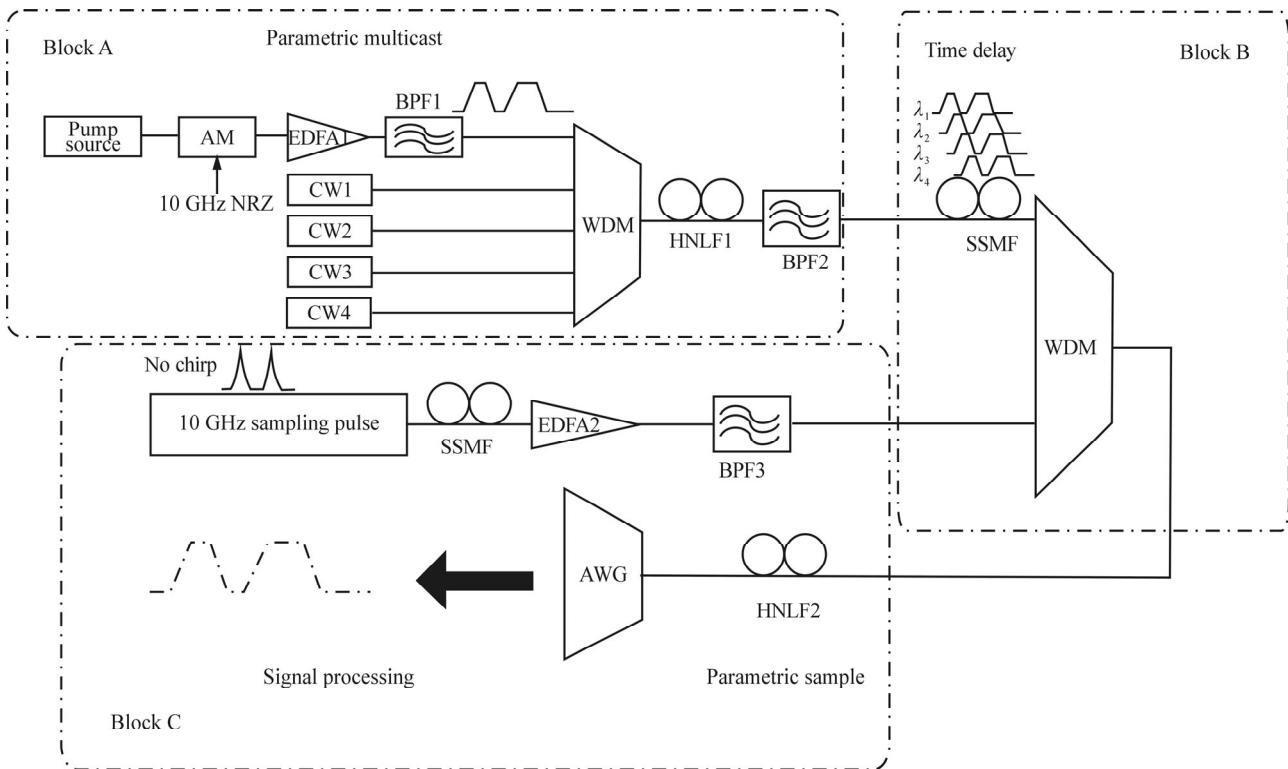


**Fig.4 Schematic diagram of optical sampling based on multicast parametric process**

The output spectra of block A are shown in Fig.5. It is evident that the 4 copies are generated at 1 558.9 nm, 1 560.8 nm, 1 562.8 nm and 1 565.0 nm, respectively. The inset of Fig.5 shows the eye diagram of Copy1.

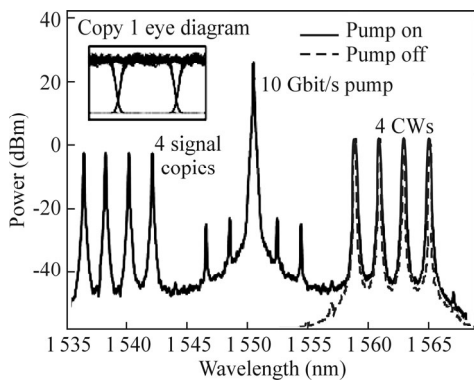


**Fig.5 The output spectra of block A (The inset shows the eye diagram of Copy1.)**

The 10 GHz original sampling pulse train and the corresponding linearly chirped ones are shown in Fig.6(a). It is evident that the original pulses are efficiently broadened in time domain after the SSMF. The FWHM of the linearly chirped pulse is 50 ps, which is about 10 times larger than that of the original pulse. The spectra of the output pulses after HNLF2 are shown in Fig.6(b). The spectral widths of idlers are obviously wider than those of copies, which agrees with our theoretical analysis shown in Fig.2(b).

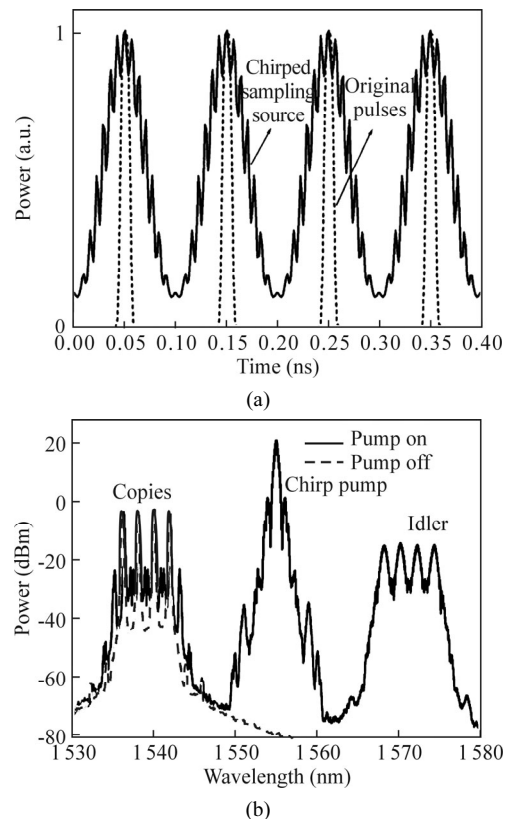


**Fig.6 (a) 10 GHz original sampling pulse train and the corresponding linearly chirped sampling pulse train; (b) The spectra of the output pulses after HNLF2**

The idlers are filtered by the AWG at 8 wavelengths

with bandwidth of 0.2 nm. The parameters are accurately configured to ensure the same time interval between 8 sampling points. The wavelengths and corresponding OSNRs are shown in Tab.1. The gain ripples of copies and the irregular shape of sampling pulses are responsible for the variation of OSNR shown in Tab.1. After AWG, the extracted sampling points are shown in Fig.7(a), which makes good agreement with the original signal shown in Fig.7(b).

**Tab.1 Wavelengths and corresponding OSNRs for 8 sample points**

Sample point	Wavelength (nm)	OSNR (dB)
Sample 1	1 568.13	43.5
Sample 2	1 568.34	43.8
Sample 3	1 570.11	42.7
Sample 4	1 570.36	42.9
Sample 5	1 572.19	43.1
Sample 6	1 572.38	43.5
Sample 7	1 574.25	43.3
Sample 8	1 574.49	43.6

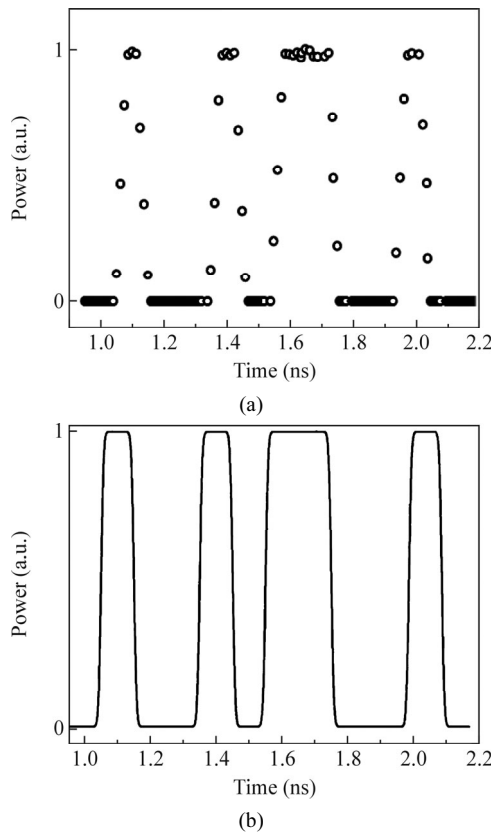


**Fig.7 (a) The extracted sampling points; (b) The waveform of the original signal**

In this paper, we propose a novel scheme for optical

real-time sampling by combining multicast parametric process and linearly chirped sampling pulses to improve the equivalent sampling rate. Simulation results show that a sampling rate of 80 Gbit/s is realized by using only one 10 GHz sampling source. The proposed scheme has good potential in high-speed optical sampling.

**References**

- [1] Yan Han and Bahram Jalali, *Journal of Lightwave Technology* **21**, 3085 (2003).
- [2] Yan Han, Ozdal Boyraz and Bahram Jalali, *IEEE Transaction Microwave Theory Techniques* **53**, 1404 (2005).
- [3] A. S. Bhushan, F. Coppinger and B. Jalali, *Electronics Letters* **34**, 839 (1998).
- [4] Hao Chi, Ying Chen, Yuan Mei, Xiaofeng Jin, Shilie Zheng and Xianmin Zhang, *Optics Letters* **38**, 136 (2013).
- [5] Hao Nan, Yuantao Gu and Hongming Zhang, *IEEE Photonics Technology Letters* **23**, 67 (2011).
- [6] Marc B. Airola, Sean R. O’Connor, Michael L. Dennis and Thomas R. Clark, *IEEE Photonics Technology Letters* **20**, 2171 (2008).
- [7] Zhe Kang, Juihui Yuan, Qiang Wu, Tao Wang, Sha Li, Xinzhu Sang, Chongxiu Wang and G. Farrell, *IEEE Photonics Journal* **5**, 7201109 (2013).
- [8] Zhe Kang, Jinhui Yuan, Sha Li, Songlin Xie, Binbin Yan, Xinzhu Sang and Chongxiu Yu, *Chinese Physics B* **22**, 114211 (2013).
- [9] Tang Dingkang, Zhang Jianguo, Liu Yuanshan and Zhao Wei, *Chinese Optics Letters* **8**, 630 (2010).
- [10] M. Westlund, P. A. Andreks, H. Sunnerud, J. Hansryd and Jie Li, *Journal of Lightwave Technology* **23**, 2012 (2005).
- [11] Camille-Sophie Brès, Nikola Alic, Alan H. Gnauck, Robert M. Jopson and Stojan Radic, *IEEE Photonics Technology Letters* **20**, 1222 (2008).
- [12] Camille-Sophie Brès, Andreas O. J. Wiberg, Bill P.-P. Kuo, Jose M. Chavez-Boggio, Christopher F. Marki, Nikola Alic and Stojan Radic, *Journal of Lightwave Technology* **28**, 434 (2010).
- [13] C.-S. Brès, A. Q. J. Wiberg, B. P. P. Kuo, N. Alic and S. Radic, *IEEE Photonics Technology Letters* **21**, 1002 (2009).
- [14] Reza Salem, Mark A. Foster, Amy C. Turner-Foster, David F. Geraghty, Michal Lipson and Alexander L. Gaeta, *Optics Express* **17**, 4324 (2009).
- [15] H. C. Hansen Mulvad, E. Palushani, H. Hu, H. Ji, M. Galili, A. T. Clausen, M. Pu, K. Yvind, J. M. Hvam, P. Jeppesen and L. K. Oxenløwe, *Optics Express* **19**, B825 (2011).